THEORETICAL AND APPLIED MECHANICS
Volume 43 (2016) Issue 1, 99–115 DOI: 10.2298/TAM160322006M

PHYSIOLOGICAL NON-NEWTONIAN BLOOD FLOW THROUGH SINGLE STENOSED ARTERY

Khairuzzaman Mamun, Mohammad Ali, and Most. Nasrin Akhter

Abstract. A numerical simulation to investigate the Non-Newtonian modeling effects on physiological flows in a three dimensional idealized artery with a single stenosis of 85% severity is given. The wall vessel is considered to be rigid. Oscillatory physiological and parabolic velocity profile has been imposed for inlet boundary condition. Determination of the physiological waveform is performed using a Fourier series with sixteen harmonics. The investigation has a Reynolds number range of 96 to 800. Low Reynolds number $k-\omega$ model is used as governing equation. The investigation has been carried out to characterize two Non-Newtonian constitutive equations of blood, namely, (i) Carreau and (ii) Cross models. The Newtonian model has also been investigated to study the physics of fluid. The results of Newtonian model are compared with the Non-Newtonian models. The numerical results are presented in terms of velocity, pressure, wall shear stress distributions and cross sectional velocities as well as the streamlines contour. At early systole pressure differences between Newtonian and Non-Newtonian models are observed at pre-stenotic, throat and immediately after throat regions. In the case of wall shear stress, some differences between Newtonian and Non-Newtonian models are observed when the flows are minimum such as at early systole or diastole. In general, the velocities at throat regions are highest at all-time phase. However, at pick systole higher velocities are observed at post-stenotic region. Downstream flow of all models creates some recirculation regions at diastole.

Nomenclature

D	Diameter of the healthy artery
L	Length of the artery
r	Radial location of the flow field
R	Radius of the healthy artery
U	Average velocity
μ	Constant viscosity of blood
LDL	Lower density Lipoprotein
PDE	Partial Differential Equation

2010 *Mathematics Subject Classification:* 76Z05, 92C35.
Key words and phrases: viscoelastic fluid, non-Newtonian, atherosclerosis.

τ	Shearing stress
γ	Shear rate
ε	Dissipation of turbulent kinetic energy
x	Axial location of the flow field
g	Acceleration due to gravity
t	Time period of the inlet flow cycle
u	Instantaneous velocity
WSS	Wall shear stress
ρ	Density of blood
3D	Three Dimension
Re	Reynolds Number
v	Kinematic viscosity of the fluid
k	Turbulent kinetic energy
UDF	User Defined Function

1. Introduction

The physiology of the cardiovascular system was studied step by step through many years. The role of the blood vessels has already been identified, when it was realized that the arteries and veins have different roles. Arteries carry blood with oxygen red blood cells, oxygen, white blood cells, nutrients, and other vital substances that the body requires from heart out to body, while veins carry blood with Carbon dioxide and various devoid of substance from body to heart. Arteries are strong, flexible blood vessels that are able to expand and contract. They expand as your heart beats, and contract between heartbeats. Veins are less flexible than arteries. Arteries contain endothelium, a thin layer of cells that keeps the artery smooth and allows blood to flow easily. Atherosclerosis starts when the endothelium becomes damaged, allowing Lower Density Lipoprotein (LDL cholesterol) to accumulate in the artery wall. The body sends macrophage white blood cells to clean up the cholesterol, but sometimes the cells get stuck there at the affected site. Over time this results in plaque being built up, consisting of bad cholesterol (LDL cholesterol) and macrophage white blood cells. This can cause severe diseases such as the development of atherosclerosis. As a result the arterial wall loses its elastic property which limits the area of blood flow. This narrowing of the artery is called arterial stenosis.

The comparison of stenosed flow behavior with the normal one can provide the proper understanding of underlying mechanism behind the development of atherosclerosis. The flow turns to be abnormal in the reduced cross sectional area of the artery stated by Kader and Shenory [1]. The flow behavior in the stenosed artery is quite different in comparison to the normal one. Stress and resistance to flow is much higher in stenosed artery. Chua and Shread [3] found that the flow through the constricted tube is characterized by high velocity jet generated at constricted region. Kader and Shenory [1] found the results from numerical simulation which demonstrated that velocity and stenotic jet length increases in increasing

the severity of stenosis. Their results also demonstrate that the 3D stenotic CFD model is capable of predicting the changes in flow behavior for increased severity of stenosis. Young et al. [4] studied the wall shear stress and pressure gradient in the stenosis and evaluated the cause of plaque rupture. The authors studied pulsatile blood flow through the stenosis with elastic wall to observe the lumen movement. According to their study the peak WSS occurred just before minimum lumen position. Pinto et al. [5] performed numerical simulation assuming a physiological pulsatile flow through different models of stenosis. In case of subject-specific anatomically realistic stenosed carotid bifurcation subjected to pulsatile inlet condition, the simulation results demonstrated the rapid fluctuation of velocity and pressure in post-stenotic region by S. Lee and S. Lee [7]. Ahmed and Giddens [6] studied both steady and pulsatile flow through 25%, 50% and 75% constriction of a rigid tube where Reynolds number ranged from 500 to 2000. In another study, the stenosis having different geometric profiles like trapezium, semi-ellipse and triangle were analyzed considering the Non-Newtonian behavior by Lorenzini and Casalena [8]. The authors investigated that the length of flow disturbance is due to stenotic shape, downstream disturbance is due to stenotic walls and peak velocity depends on the shape of stenosis.

A number of studies were done to observe the effect of stenosis when blood flows through the stenosis of the artery, assuming blood as Newtonian. But the assumption of Newtonian behavior of blood is acceptable for flow in large arteries, and of high Reynolds number and high shear rate stated by Rabby et al. [2]. In case of pulsatile blood flow there are some moments (like diastole, early systole) when blood flow has low Reynolds number. Again in various arteries there are some constrictions called stenosis where blood flow has low Reynolds number or low shear rate. But when shear rate is low (less than $100\,\mathrm{s}^{-1}$, the Non-Newtonian behavior of blood flow is acceptable stated by Rabby et al. [2]. It was also revealed that some diseased condition like severe myocardial infarction, cerebrovascular diseases and hypertension, blood exhibits remarkable Non-Newtonian properties by Chien [9]. According to Berger and Jou [10], if the shear rate is high, the blood behaves like a Newtonian fluid whose viscosity be $0.00345\,\mathrm{Pa}\cdot\mathrm{s}$. However, if the Reynolds number or shear rate of blood flow falls down due to various diseased conditions, its viscosity increases and blood exhibits Non-Newtonian property. In most cases, though, Non-Newtonian blood models would provide a more accurate representation of blood flow behavior within the arteries of interest, particularly for stenosed conditions. Studies had documented three types of Non-Newtonian blood properties: thixotropy, viscoelasticity and shear thinning. Thixotropy is a transient property of blood, which is exhibited at low shear rates and has a fairly long time scale. Mandal [11] suggested that this indicates a secondary importance in physiological blood flow. Mandal further explained, based on the research by Thurston [12, 13], that blood contains a number of particles and cells suspended within the flow that interact with each other significantly as to complicate two-phase modeling. Blood therefore exhibits significant viscoelastic properties, which is also a transient condition at the frequency range of common physiological condition. This has attracted significant research interest trying to determine useful

mechanical properties to be employed in analytical calculations and simulations. Mandal [11], noted that the viscoelastic property of blood diminishes vary rapidly as shear rate rises. At physiological hematocrit values, which is the volume fraction of red blood cells in whole blood, this effect is not significant, suggesting that this Non-Newtonian behavior is of secondary importance for normal pulsatile blood flow. Mandal [11] therefore concluded that shear thinning is the dominant characteristic of blood. Studies had therefore attempted to fit experimentally measured blood flow behavior to shear thinning equations with modifications to take into account the hematocrit values in Cho and Kensey [14]; Walawender et al. [15]; Cokelet et al. [16]; Powell and Eyring [17]. A common property of these shear thinning equations was that the effective viscosity of the blood drops in regions of high shear rates and vice versa. From these studies several models were derived and validated against experimentally derived blood flow properties.

There have been numerous simulations that have incorporated Newtonian, Non-Newtonian blood flow through single stenotic artery individually. However, there has been little research into combining all of the above conditions together. This study aims to incorporate the Newtonian & Non-Newtonian pulsatile flow through single stenosis to investigate the flow characteristics. Two Non-Newtonian models have been investigated, Carreau model and Cross model, to determine their respective Non-Newtonian influences. Finally, an attempt has been made in this study to demonstrate the significant changes of flow behavior through the stenotic arteries.

2. Model description

2.1. Geometry. Three dimensional stenotic arteries are used as geometry for this study shown in Fig. 1(a). For this study, 85% stenotic artery (by area) is taken as geometry. The geometry of generated model in this study has a diameter (D) of 6 mm and a length (L) of 96 mm, where the length of pre stenotic, throat and post stenotic region are $4D$, $2D$ and $10D$ respectively. The wall is considered to be rigid. The flow field mesh consists of of 45496 nodes and 95592 elements for the geometry. Figure 1(b) shows the mesh in cross sectional inflow plane of the stenotic artery.

FIGURE 1. (a) Model of a stenotic artery; (b) mesh in cross sectional inflow plane of a stenotic artery.

2.2. Blood properties. The density of the blood is $1050\,\mathrm{kg/m^3}$. In a Newtonian model for the blood viscosity, the value of μ is treated as a constant usually set to $\mu = 3.45\times10^{-3}\,\mathrm{Pa{\cdot}s}$. But when blood is considered non-Newtonian fluid then the viscosity of the blood is calculated from two models such as Carreau model and Cross model.

2.2.1. *Cross model for the non-Newtonian blood viscosity.* For non-Newtonian fluid Malcolm M. Cross [20] proposed a shear rate dependent viscosity model called Cross model. The Cross model is defined by

$$\mu = \mu_\infty + (\mu_0 - \mu_\infty)\left[1 + \left(\frac{|\gamma|}{\gamma_c}\right)^m\right]^{-1}$$

where, $\mu_0 = 0.0364\,\mathrm{Pa{\cdot}s}$ is the usual molecular blood viscosity when very zero shear rates, $\gamma_c = 2.63\,\mathrm{s^{-1}}$ is the reference shear rate, $\dot\gamma$ is the instantaneous shear rate, and $m = 1.45$ is the constant.

2.2.2. *Carreau model.* the Carreau model is defined by Pierre Carreau [21] $\mu = \mu_\infty + (\mu_0 - \mu_\infty)[1 + (\gamma_c\dot\gamma)^2]^{n-1/2}$ where $\mu_\infty = 0.00345\,\mathrm{Pa{\cdot}s}$, $\mu_0 = 0.056\,\mathrm{Pa{\cdot}s}$, $\gamma_c = 3.313\,\mathrm{s}$, $\dot\gamma$ is the instantaneous shear rate, and $n = 0.3568$.

3. Governing equation and boundary condition

3.1. Governing equation. Due to constriction, blood passes through the throat and post stenotic region with high velocity. Flow velocity at post stenotic region increases but pressure of that region decreases. So, moderate and severe arterial stenosis restricts the flow severely with creating turbulent flow characteristics. For this region, turbulent flow is expected at post stenotic region especially for 85% stenotic artery. Neither laminar flow modeling nor standard two-equation models are suitable for this kind of blood flow. So, Wilcox low-Re turbulence model is more acceptable for flow analysis found by Varghese and Frankel [19]. Therefore, low Re $k-\omega$ turbulent mode is taken for calculation.

Now, the Navier–Stokes equation can be given by:

$$\frac{\partial u_i}{\partial x_i} = 0$$

$$\frac{\partial u_i}{\partial t} + u_j\frac{\partial u_i}{\partial x_j} = -\frac{1}{\rho}\frac{\partial p}{\partial x_i} + \frac{\partial^2 u_i}{\partial x_j \partial x_i}$$

Since each term of this equation is time averaged, the equation is referred to as a Reynolds averaged Navier–Stokes (RANS) equation. During this procedure, several additional unknown parameters appear which require additional equations to be introduced as turbulence models. The set of RANS equations are:

$$\frac{\partial \rho}{\partial t} + \frac{\partial(\rho u_i)}{\partial x} = 0$$

$$\frac{\partial(\rho u_i)}{\partial t} + \frac{\partial(\rho u_i u_j)}{\partial x_j} = -\frac{\partial p}{\partial x_i} + \frac{\partial}{\partial x_j}\left[\mu\Big(\frac{\partial u_i}{\partial x_j} + \frac{\partial u_j}{\partial x_i} - \frac{2}{3}\delta_{ij}\Big(\frac{\partial u_1}{\partial x_1}\Big)\Big)\right] + \frac{\partial}{\partial t}(-\rho\overline{u_i' u_j'})$$

In this equation $-\rho\overline{u_i' u_j'}$ is an additional term known as the Reynolds's stress tensor, which can be approximated by using Boussinesq's hypothesis:

$$-\rho\overline{u_i'u_j'} = \mu_t\Big(\frac{\partial u_i}{\partial x_j} + \frac{\partial u_j}{\partial x_i}\Big) - \frac{2}{3}\Big(\rho k + \mu_t\frac{\partial u_k}{\partial x_k}\Big)$$

Eddy viscosity can be modeled as a function of the turbulence kinetic energy k and specific dissipation rate ω; therefore it is referred to as the two-equation turbulent model.

The turbulence kinetic energy k and specific dissipation rate ω of standard $k-\omega$ model are determined by following two equations:

$$\frac{\partial}{\partial t}(\rho k) + \frac{\partial}{\partial x_i}(\rho k u_i) = \frac{\partial}{\partial x_j}\Big(\Gamma_k\frac{\partial k}{\partial x_i}\Big) + G_k - Y_k + S_k \qquad \text{The } k \text{ equation}$$

$$\frac{\partial}{\partial t}(\rho \omega) + \frac{\partial}{\partial x_i}(\rho \omega u_i) = \frac{\partial}{\partial x_j}\Big(\Gamma_\omega\frac{\partial k}{\partial x_i}\Big) + G_\omega - Y_\omega + S_\omega \qquad \text{The } \omega \text{ equation}$$

In these equations, G_k represents the generation of turbulence kinetic energy due to mean velocity gradients. G_ω represents the generation of ω. Γ_k and Γ_ω represent the effective diffusivity of k and ω, respectively. Y_k and Y_ω represent the dissipation of k and ω due to turbulence. S_k and S_ω are user-defined source terms.

A low Reynolds number correction factor controls the influence on the overall structure of the flow field, depending upon local conditions, and it is given as

$$\alpha^* = \alpha^*_\infty\Big(\frac{\alpha^*_0 + \mathrm{Re}_t/R_k}{1 + \mathrm{Re}_t/R_k}\Big)$$

where, $\mathrm{Re}_t = \frac{\rho k}{\mu\omega}$, $R_k = 6$, $\alpha^*_0 = \frac{\beta_i}{3}$, $\beta_i = 0.072$, $\alpha^*_\infty = 1$. Closure Coefficient for the Transitional $k-\omega$ Model are $\alpha^*_\infty = 1$, $\alpha_\infty = 0.52$, $\alpha_0 = 0.1111$, $\beta^*_\infty = 0.09$, $\beta_i = 0.072$, $R_k = 6$, and $R_\beta = 8$.

3.2. Boundary condition. Since the blood flow through arterial stenosis is an unsteady phenomenon and the blood flow to be fully developed at inlet region, Oscillatory physiological parabolic velocity profile has been imposed for inlet boundary condition. For this purpose an User Defined Function (UDF) has been written in `C++` programming language to demonstrate the unsteady parabolic nature of velocity profile using the relation given by the following equations, $u_x = u\big(1-\frac{y^2+z^2}{\text{radius}^2}\big)$, where $u = \sum_{n=0}^{n=16}(a_n\cos(\omega t) + B_n\sin(\omega t))$. A_n and B_n are the coefficients.

TABLE 1. Harmonic coefficients for pulsatile waveform shown in Figure 2(a).

n	A_n	B_n	n	A_n	B_n	n	A_n	B_n
0	0.166667	0	6	-0.01735	0.01915	12	-0.00341	0.005463
1	-0.03773	0.0985	7	-0.00648	0.002095	13	-0.00194	0.000341
2	-0.10305	0.012057	8	-0.01023	-0.0078	14	-0.00312	-0.00017
3	0.007745	-0.06763	9	0.008628	-0.00663	15	0.000157	-0.00299
4	0.025917	-0.02732	10	0.002267	0.001817	16	0.001531	0.000226
5	0.037317	0.024517	11	0.005723	0.003352			

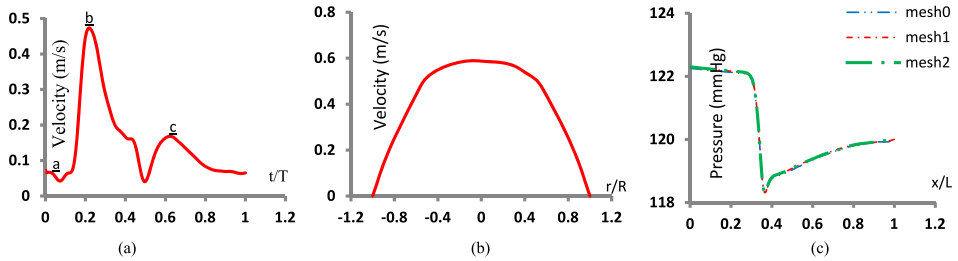

FIGURE 2. (a) Oscillatory physiological waveform, (b) parabolic inlet velocity profile, and (c) pressure distribution in 65% stenotic artery from different mesh sizes.

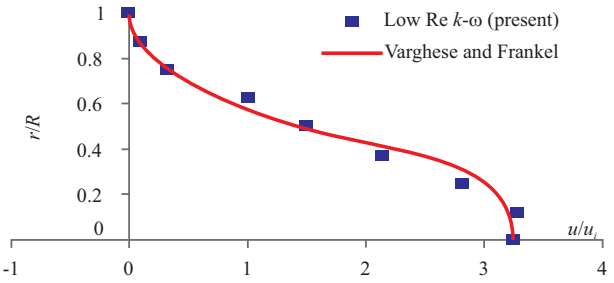

FIGURE 3. Comparison of computed steady velocity profile.

Detailed descriptions of sixteen harmonic coefficients are shown in Table 1. Here, Reynolds number varies from 96 to 800. Since cardiac pulse cycle is 0.82 sec, ω is found from the calculation $\omega = \frac{2\pi}{0.82} = 7.66$ rad/sec. Figure 2(a) and 2(b) show oscillatory physiological waveform and parabolic inlet velocity profile respectively. In Figure 2(a), $\underline{a}$, $\underline{b}$, and $\underline{c}$ represent the positions of early systole (0.041 sec), peak systole (0.205 sec), and diastole (0.615 sec) respectively.

3.3. Grid independence check. An extensive test is carried out with different sizes of mesh such as mesh0 (75511 element), mesh1 (82580 element) and mesh2 (90227 element) respectively. Figure 2(c) shows the pressure distributions for 65% stenosis artery with mentioned mesh sizes. In all cases, the pressure distributions are same. It implies that the solution is grid independence.

3.4. Validation. Before starting of present investigation the numerical simulation is needed to be validated. Validation of the present numerical computation is done by plotting the steady velocity profile at 2.5D downstream from the stenosis throat and comparing it with the velocity profile of Varghese and Frankel [19]. For this case, a parabolic velocity profile is assumed as inlet boundary condition. The mean inlet velocity corresponds to Reynolds number 500 and the flow is assumed to be steady. The results are shown in the Figure 3, where a good agreement can be found with Varghese and Frankel [19].

4. Numerical scheme

The numerical simulations are performed by well-known software ANSYS Fluent 14.5. A pressure based algorithm is chosen as the solver type. This solver is generally selected for an incompressible fluid. As there is no heat transfer in the blood flow process, energy equation is not solved. Since turbulent is expected in 85% stenotic artery at post stenotic region, a low Reynolds number $k-\omega$ turbulent model is used throughout the work. In solution methods, the SIMPLE algorithm is selected for pressure-velocity coupling. First Order Upwind scheme is employed as a numerical scheme for discretization of the momentum equation. The time step is set to 0.00041 sec with 2000 number of total time steps. Maximum 10 iterations are performed per each time step.

5. Results and discussion

The computational results are conducted to study the influence of stenosis on the flow behavior. The flow parameters like velocity, pressure, WSS and streamline are observed from longitudinal contours at specific instants of pulse cycle for comparing the flow variation. The discussion is categorized with the observations of flow variation starting from early systole, peak systole and diastole, respectively.

It is known that blood is Bingham plastic fluid. So the viscosity of blood decreases with increase in share rate. When shear rate is greater than 100 then viscosity of blood is constant. The viscosity of Newtonian model is less than that of Non-Newtonian model when shear rate is less than 100, but viscosity of all models is equal when shear rate is equal to or greater than 100. When Reynolds number is very low then pressure and WSS of Newtonian model should be less than that of Non-Newtonian model but opposite scenario should be seen for velocity distribution. Since there are comparatively low Reynolds numbers at early systole and diastole, the results of Newtonian and Non-Newtonian condition should be different at early systole and diastole. On the other hand maximum Reynolds number is seen at peak systole. So the results of Newtonian and Non-Newtonian condition should follow each other at peak systole. Again the velocity of the throat region is high for any time instant. So the results of Newtonian and Non-Newtonian condition should be same at the throat region but different at the pre and post stenotic region. The results of pressure, WSS, and velocity distribution are discussed with respective figure.

5.1. Pressure distribution. Figure 4(a), 4(b), and 4(c) reveal the centerline pressure distribution for Non-Newtonian (Carreau and Cross) and Newtonian models at early systole, peak systole and diastole respectively. At early systole significant pressure difference between Newtonian and Non-Newtonian models are observed at pre stenotic, throat and post stenotic region. Pressure of the Non-Newtonian (Carreau and Cross) models are higher than that of Newtonian model which is natural and meets our expectation. Very small pressure fall at the throat region and very quick recovery of pressure after the throat region are observed. Due to high Reynolds number or high shear rate at peak systole, viscosity of Carreau, Cross and Newtonian model are same. Thus, pressure of the Non-Newtonian

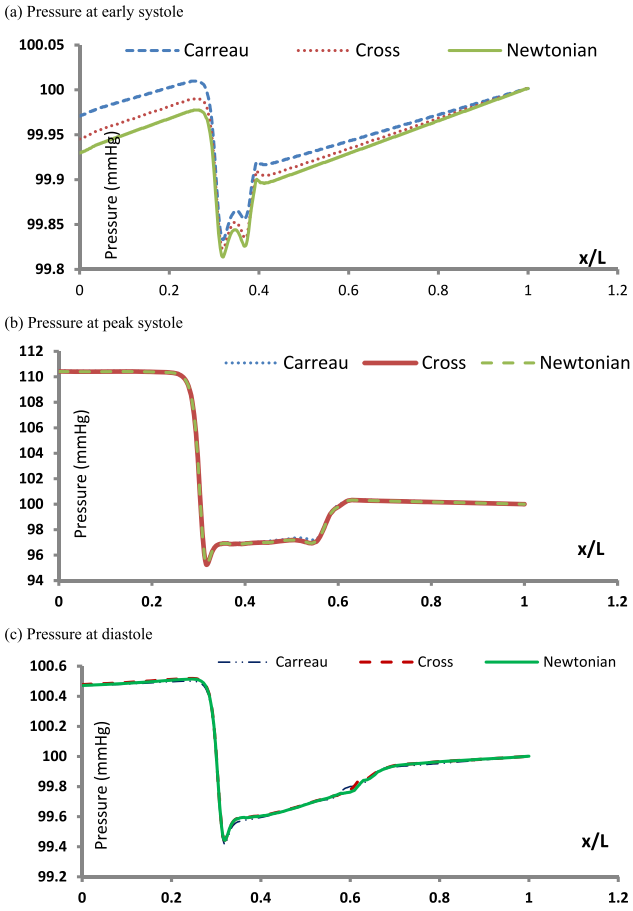

FIGURE 4. Distribution of pressure for Carreau, Cross, and Newtonian model at (a) early systole (b) peak systole and (c) diastole.

(Carreau and Cross) models follow the pressure of the Newtonian model. A very large pressure fall is noticed at the throat region, and it continues after the throat region. So peak systole is very dangerous time instant for 85% stenotic severity. At diastole pressure of the Cross model mostly follow the pressure of the Newtonian model but very little difference is observed in Carreau model. No significant pressure fall is occurred due to very low Reynolds number.

5.2. Wall shear stress distribution. Wall Shear Stress (WSS) is an important parameter to apprehend the condition of severity of arterial stenosis. It is also responsible for the growth of arterial diseases. WSS is defined as $\tau = \mu \frac{du}{dr}$, where μ is the viscosity and $\frac{du}{dr}$ is the velocity gradient. So, WSS of Non-Newtonian fluid depends on the viscosity of the fluid and velocity gradient but WSS of Newtonian fluid does not depend on the viscosity because viscosity is a constant property

of Newtonian fluid. Thus the results of WSS for Newtonian and Non-Newtonian model may be different.

Figure 5(a), 5(b), and 5(c) represent the distribution of wall shear stress for Non-Newtonian (Carreau & Cross) and Newtonian model at early systole, peak systole and diastole respectively. The wall shear stress distributions for all models are fairly similar. The difference in WSS magnitude is dependent on Reynolds number; therefore the largest difference occurs during the minimum flow such as early systole or diastole. More critically, at early systole and diastole the Carreau and Cross model are found to have a slightly higher wall shear stress distribution than the Newtonian model at the pre and post stenotic regions due to low Reynolds number or high viscosity. This is more noticeable in the regions away from the stenosis. Again results of all models are same at the throat region because of high Reynolds number or low viscosity. At peak systole the results in WSS for all models follow each other because of high Reynolds number.

Distribution of WSS exhibits the opposite scenarios of distribution of pressure. A significant increase in WSS at the throat and post-stenotic regions is observed. This increase is occurred due to the stenosis of artery which creates high shear stress on the surface of the wall. Maximum WSS is observed at pick systole because of high Reynolds number. Some fluctuations in WSS are noticed after the constriction region from Figures 5(b) and 5(c).

5.3. Velocity distribution. Figure 6(a), 6(b), and 6(c) represent the centerline velocity distribution for Non-Newtonian (Carreau & Cross) and Newtonian model at early systole peak systole and diastole respectively. At early systole it is found that the velocity profiles of Cross model mostly follow the profiles of the Newtonian model throughout the geometry but Carreau model gives slightly greater value than Newtonian model at pre and post stenotic region. The result is abnormal and not expected because velocity of Newtonian model always be equal or greater than that of Non-Newtonian model. Peak systolic velocity for all model are same at pre stenotic region due to high Reynolds number. Velocity of Cross and Newtonian model are almost same at all-time instant but some abnormal differences are seen between carreau and Newtonian model. The downstream velocity magnitude of Carreau and Newtonian model varies from each other at peak systole and diastole.

For clear interpretation of velocity distribution we need to observe different cross-sectional velocity distribution at early systole, peak systole and diastole. For this reason we have presented different cross-sectional velocity distribution at early systole, peak systole and diastole in Figure 7, 8 and 9 respectively. Figure 7 shows the cross-sectional velocity profiles at five different axial positions for Carreau, Cross, and Newtonian model at early systole. The simulation is started from the inlet and end with the outlet. In between there are three positions such as pre stenotic region, throat, and post stenotic region for the simulation. From the simulation result it is observed that velocity profile of Carreau, Cross and Newtonian model are same at inlet and throat region because blood enter with same velocity through inlet and get high velocity at throat region. Centerline velocity profile of Carreau model has a slightly greater than that of Cross and Newtonian model at pre-stenotic and outlet region. The result is abnormal for Carreau model because

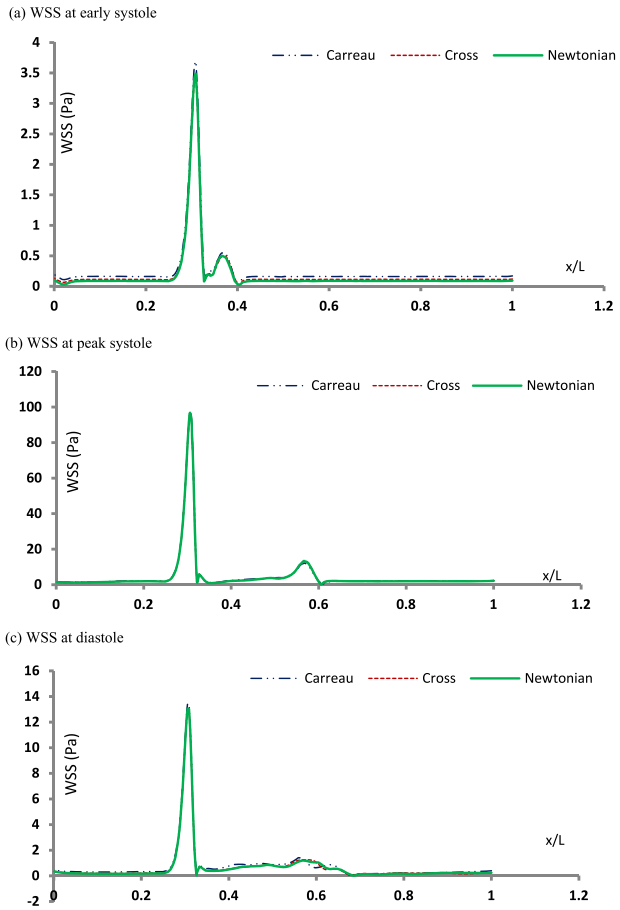

FIGURE 5. Distribution of wall shear stress for Carreau, Cross, and Newtonian model at (a) early systole (b) peak systole and (c) diastole.

velocity of Newtonian model always is equal or greater than that of Non-Newtonian model. But expected result is observed at post-stenotic region as centerline velocity profile of Carreau model is smaller than that of Cross and Newtonian model. Here Cross model gives very natural, normal and expected results such as velocity profile for Cross and Newtonian model are mostly same in magnitude at all positions.

Figure 8 represent same results at peak systole. Since at peak systole Reynolds number or shear rate is high, blood acts as Newtonian fluid. So the results for all models should be equal. Thus velocity profile for all model are almost same except the post-stenotic region. At post-stenotic region centerline velocity profile of Carreau model is a slightly smaller than that of Cross and Newtonian model. Figure 9 shows the cross-sectional velocity profiles at five different axial positions for Carreau, Cross, and Newtonian model at diastole. It is observed that velocity profile of Carreau, Cross and Newtonian model are same at inlet and throat region.

Centerline velocity profile of Carreau and Cross model have a slightly smaller magnitude than Newtonian model at pre-stenotic region. At post-stenotic region centerline velocity for Carreau model is smaller than Cross and Newtonian model but velocity for Cross and Newtonian model are same. Different and abnormal Centerline velocities for all models are observed at outlet.

5.4. Streamline contours. Variations of streamlines contours have been investigated for Carreau, Cross, and Newtonian model to study the flow pattern of blood through the stenotic artery. Streamline distribution for the models at early-systole, peak-systole, and diastole is shown in Figure 9, 10, and 11 respectively. At early systole there is no vortex in Carreau, and Cross model and streamlines

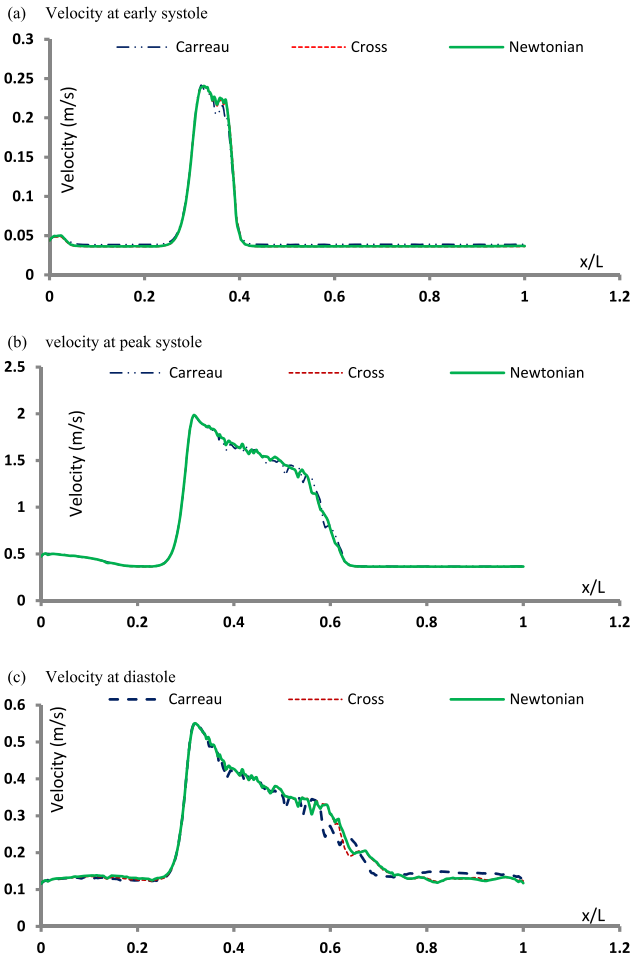

FIGURE 6. Distribution of velocity for Carreau, Cross, and Newtonian model at (a) early systole (b) peak systole and (c) diastole.

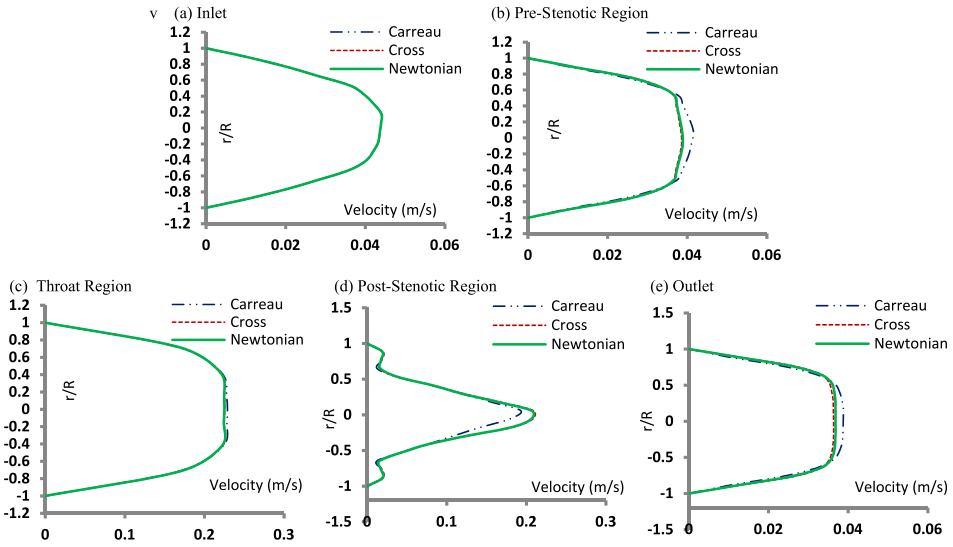

FIGURE 7. Velocities at different axial positions for Carreau, Cross, and Newtonian model at early systole.

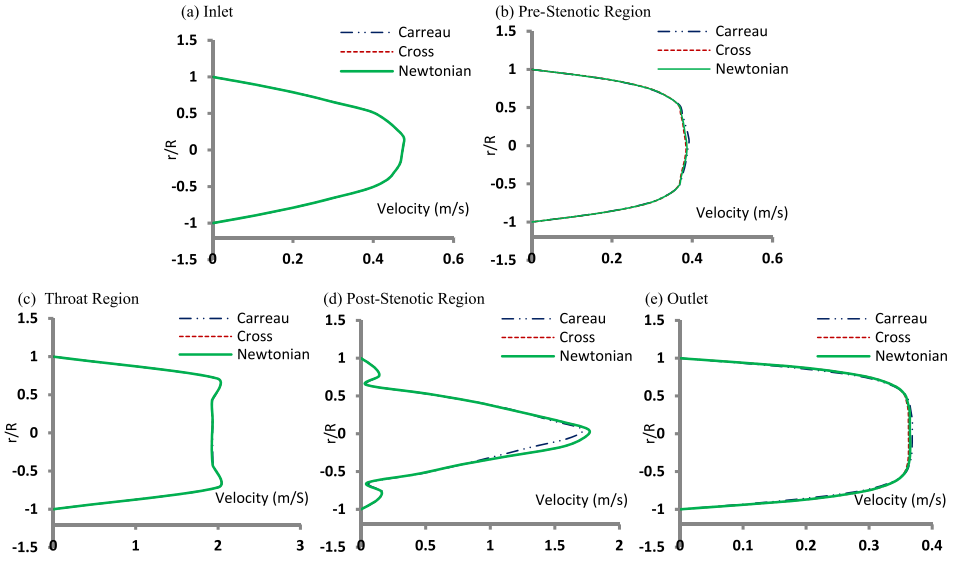

FIGURE 8. Velocities at different axial positions for Carreau, Cross, and Newtonian model at peak systole.

run smoothly throughout the geometries. But in Newtonian model a very small vortex is noticed near the throat, except this most of the streamlines run smoothly throughout the geometry. At peak all models create vortex. Two large vortexes at the post stenotic region near the throat are seen in all models. But there are differences in vortex size and shape. Vortexes are almost same for Cross and Newtonian model but Carreau model is different from them. In Carreau model vortexes are large in size and shape than Cross and Newtonian model. At diastole all models create significant size of vortex. Length of vortex is increased in Cross and Newtonian model. Significant streamline differences are observed among the models. Carreau model create large difference in streamline from Cross and Newtonian models. But slightly small difference in streamline distribution are seen between Cross and Newtonian model.

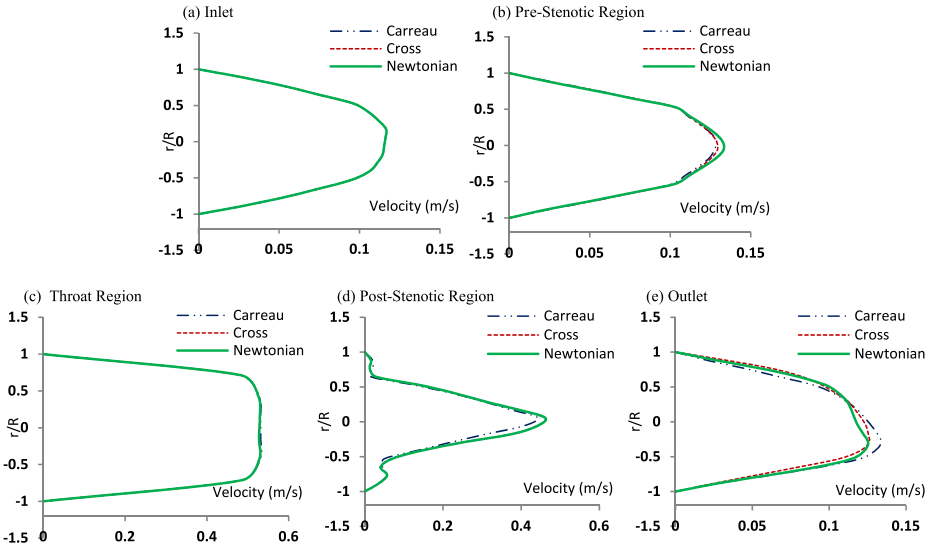

FIGURE 9. Velocities at different axial positions for Carreau, Cross, and Newtonian model at diastole.

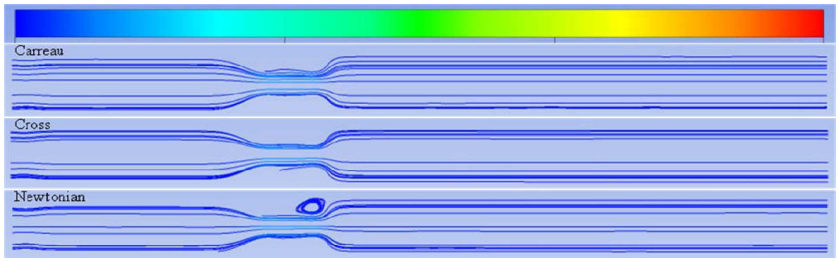

FIGURE 10. Streamlines contours for Carreau, Cross, and Newtonian model at early systole.

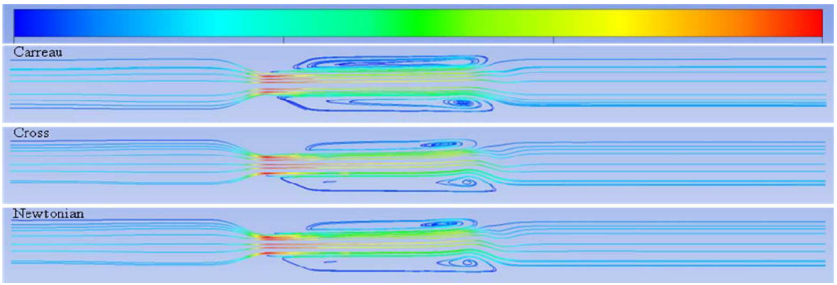

FIGURE 11. Streamlines contours for Carreau, Cross, and Newtonian model at peak systole.

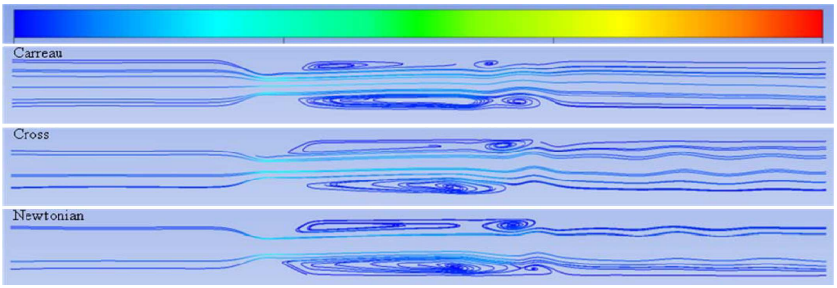

FIGURE 12. Streamlines contours for Carreau, Cross, and Newtonian model at diastole.

6. Conclusion

Many studies have been taken experimentally and theoretically treating blood as Newtonian fluid but in this paper blood is assumed as both Newtonian and Non-Newtonian for a comparative study among the model. It is noticed that largest difference in wall shear stress occurs during the minimum flow such as early systole or diastole. At early systole the magnitude of pressure for Carreau model is higher than Cross and Newtonian model but result for Cross model is also higher than Newtonian model. In velocity distribution it is found that the velocity profiles of Cross model mostly follow the profiles of the Newtonian model but differ from the Carreau model. The results of the cross sectional velocity and streamline distribution describe that Cross model gives mostly same results of Newtonian model. Therefore, in comparison Cross model gives better results than other model.

References

1. S. Khader, B. Shenoy, *Effect of increased severity in patient specific stenosis*, World Journal of Modelling and Simulation **7**(2) (2011), 113–122.
2. M. G. Rabby, A. Razzak, Md. M. Molla, *Pulsatile non-Newtonian blood flow through a model of arterial stenosis*, Procedia Engineering **56** (2013) 225–231.
3. C. S. Chua, G. J. Sheard, K. Ryan, A. Fouras, *Changes in flow and wall stresses through arterial constriction offset from the centre of the vessel*, ANZIAM J. **50** (2009), C744—C759.

4. V. Young, A. Patterson M. Graves, Z-Y LI, V. Tavani, T. Tang, J. H. Gillard, *The mechanical triggers of rupture: shear vs pressure gradient*, Br. J. Radiol. **82** (2009) S39–S45.
5. J. Pinto, K. L. Bessa, D. F. Legendre, R. H. Mouth, *Physiologycal pulsatile waveform through axisymmetric stenosed arteries: Numerical Simulation*, ABCM Symposium in Bioengineering **1** (2006), I.02.
6. S. A. Ahmed, D. P. Giddens, *Pulsatile Poststenotic Flow Studies with Laser Doppler Anemometry*, J. Biomech. **17** (1984), 695–705.
7. S. Lee, S. Lee, *Direct numerical simulation of transitional flow in a stenose carotid bifurcation*, J. Biomech. **41** (2008), 2551–2561.
8. G. Lorenzini, E. Casalena, *CFD analysis of pulsatile blood flow in an atherosclerotic human artery with eccentric plaques*, J. Biomech. **41** (2008), 1862–1870.
9. Chien, S., *Hemorheology in clinical medicine*, Recent Advances in Cardiovascular Diseases **2** (Suppl.) (1981), 21–26.
10. S. A. Bereger, L. D. Jou, *Flows in stenotic vessels*, Annu. Rev. Fluid Mech. **32** (2002), 347–382.
11. P. K. Mandal, *An unsteady analysis of non-Newtonian blood flow through tapered arteries with a stenosis*, Int. J. Non-Linear Mech. **40** (2005), 151–164.
12. G. B. Thurston, *Viscoelasticity of human blood*, J. Biophys. **12** (1972), 1205–1212.
13. G. B. Thurston, *Frequency and shear rate dependence of viscoelasticity of human blood*, Biorheology **10** (1973), 375–381.
14. Y. I. Cho, K. R. Kensey, *Effects of the non-Newtonian viscosity of blood in flows in a diseased arterial vessel. Part 1: Steady flows*, Biorheology **28** (1991), 241–262.
15. W. P. Walawender, T. Y. Chen, D. F. Cala, *An approximate Casson fluid model for tube flow of blood*, Biorheology **12** (1975), 111–119.
16. G. R. Cokelet, *The rheology of the human blood. Chapter 4 in Biomechanics: Its Functions and Objectives*, in: Y. C. Fun, N. Perrone, M. Anliker (eds.) Prentice–Hall, Englewood Cliffs, 63–103, 1972.
17. R. E. Powell, H. Eyring, *Mechanism for Relaxation Theory of Viscosity*, Nature **154** (1944), 427–428.
18. K. Mamun, M. N. Akhter, M. S. H. Mollah, M. A. N. Sheikh, M. Ali, *Characteristics of pulsatile blood flow through 3-D geometry of arterial stenosis*, Procedia Engineering **105** (2015), 877–884.
19. S. S. Varghese, S. H. Frankel, *Numerical Modeling of Pulsatile Turbulent Flow in Stenotic Vessels*, J. Biomech. **125** (2003), 445–460.
20. M. M. Cross, *Rheology of non-Newtonian fluids: a new flow equation for pseudoplastic systems*, Journal of Colloid Science **20**(5) (1965), 417–437.
21. P. J. Carreau, *Rheological equations from molecular network theories, Transactions of The Society of Rheology (1957-1977)*, 1972 - scitation.aip.org

ФИЗИОЛОШКИ НЕ-ЊУТНОВ ПРОТОК КРВИ КРОЗ АРТЕРИЈУ СА ЈЕДНИМ СУЖЕЊЕМ

Резиме. Дата је нумеричка симулација не-Њутновских модела физиолошких токова у идеализованој тродимензионалној артерији са једним сужењем од 85%. Зид артерије је сматран крутим. Колебање физиолошког и параболичног профила брзина је одређено у зависности од почетних граничних услова. Одређивање физиолошког таласа је урађено помоћу Фуријеовог реда са шеснаест хармоника. Истраживан ток има Рејнолдсов број у распону од 96 до 800. Систем је описан помоћу $k-\omega$ модела са малим Рејнолдсов бројем. Истраживање је спроведено ради карактеризације двају не-Њутновских конститутивних једначина тока крви: (i) Carreau и (ii) Cross модела. Такође, за проучавање физике флуида, коришћен је и Њутновски модел. Резултати Њутновског модела су упоређени са не-Њутновским моделима. Нумерички резултати су дати у зависности од брзине, притиска, дистрибуцијом смичућих напона на зиду артерије, попречним пресеком брзина, као и контуре струјних линија. У раној систоли разлике притисака између Њутновог и не-Њутновских модела су уочене пре сужњења и у области одмах након сужења. Узимајући у обзир смичући напон на зиду артерије, разлике између Њутновог и не-Њутновских модела су примећене када су токови минимални, као што је у раној систоли или дијастоли. Уопште, брзине у регионима сужења су највеће у свим фазама. Међутим, у врхунцу систоле веће брзине су уочене у области после сужења. Низ струјање, ток свих модела ствара рециркулационе области у дијастоли.

Department of Mathematics
Dhaka University of Engineering and Technology
Gazipur
Bangladesh

Department of Mechanical Engineering
Bangladesh University of Engineering and Technology
Dhaka
Bangladesh

Department of Mathematics
Dhaka University of Engineering and Technology
Gazipur
Bangladesh
nasrin@duet.ac.bd

(Received 22.03.2016)
(Revised 09.06.2016)
(Available online 24.06.2016)